Natural convection in air layers between horizontal concentric isothermal cylinders

Samy M. El-Sherbiny and Atef R. Moussa
Mechanical Eng. Dept., Faculty of Eng., Alexandria University, Alexandria, Egypt

Natural convection in air between two infinite horizontal concentric cylinders at different constant temperatures is numerically investigated. The study covered a wide range of the Rayleigh number, Ra from 10^2 to 10^6, and the Radius Ratio, (RR) was changed between 1.25 and 10. The differential governing equations (mass, momentum, and thermal energy together with their boundary conditions) were solved using a finite difference method. The numerical method and the computer program are checked for the case of pure conduction. The results were presented graphically in the form of streamlines and isotherms. The local and average Nusselt numbers, velocities and temperature distributions are also presented. The flow starts in the conduction regime at low Rayleigh numbers ($Ra \leq 10^2$) and low radius ratios. It changes to the laminar boundary layer regime as the Rayleigh number or the radius ratio was increased. The study showed that the average Nusselt number increased with the increase of each of Ra and RR in the laminar boundary layer regime. For any fixed value of Ra, the laminar convection starts earlier at higher values of the radius ratio. The annular gap will act as a single inner cylinder in an infinite medium at RR= 10 for $Ra \leq 10^5$. For $Ra > 10^5$, the radius ratio has to be increased much over RR=10 in order for the annular gap to behave as a single cylinder. The numerical results were correlated as a function of Ra and RR. A good agreement is shown between the present correlation and previous data and correlations. The present correlation lies between the other correlations with a maximum deviation of 9.6 %.

تم عمل دراسة عددية للحمل الحر بين إسطوانتين أفقيتين لا نهائيتين ومتحدتى المحور عند درجتى حرارة مختلفتين . وقد شملت الدراسة مدى واسع لرقم رالى بين ١٠^{٢} ، ١٠^{٦} وتغيرت النسبة بين قطرى الاسطوانتين بين ١,٢٥ ، ١٠ . وقد تم حل المعادلات التفاضلية التى تحكم تبادل الكتلة وكمية الحركة والطاقة باستخدام الطرق العددية باستخدام برنامج حاسب ألى بعد إختباره فى حالة إنتقال الحرارة بالتوصيل فقط . تم عرض النتائج فى منحنيات تعبر عن خطوط السريان ودرجة الحرارة . كما تم عرض النتائج المعبرة عن رقم نوسلت الموضعى والمتوسط وكذلك توزيعات درجة الحرارة والسرعة . عندما تكون النسبة بين قطرى الاسطوانتين صغيرة ورقم رالى أقل من ١٠^{٢} فإن الحرارة تنتقل اساسًا بالتوصيل وتتغير الحالة إلى السريان الجدارى الرقائقى عند زيادة نسبة القطرين أو رقم رالى . وقد أظهرت الدراسة أن رقم نوسلت المتوسط يزداد مع زيادة كل من نسبة القطرين و رقم رالى فى حالة السريان الجدارى الرقائقى . كما أن الاسطوانة الداخلية يمكن أن تعامل كما لو كانت أسطوانة مفردة فى وسط لانهائى عندما تكون نسبة القطرين = ١٠ ورقم رالى أقل من ١٠^{٥} . وعند زيادة رقم رالى عن ١٠^{٥} فإن نسبة القطرين فى هذه الحالة يجب أن تزيد كثيرًا عن ١٠ . وقد تم إستنتاج معادلة تمثل النتائج العددية وقد أظهرت توافقاً كبيرًا مع النتائج السابقة وكانت فى وضع وسط بينها وكان أقصى إختلاف موجود فى حدود ٩,٦ ٪ .

Keywords: Natural convection, Air layers, Horizontal cylinders, Annular gaps

1. Introduction

Natural convection in a horizontal annulus kept at constant surface temperatures has been the subject of interest of many researchers due to its theoretical interest and its various engineering applications such as solar collectors design, thermal storage systems, nuclear reactors, cooling of electronic components, aircraft fuselage insulation, under ground electrical transmission lines, etc.

Extensive survey on natural convection between two horizontal concentric cylinders is given by Kuehn and Goldstein [1]. They performed both experimental and theoretical-numerical studies for air and water at Rayleigh numbers (based on gap width, *L*) from 2.1×10^4 to 9.8×10^5 at a diameter ratio of 2.6. A numerical parametric study was carried out by Kuehn and Goldstein [2], in which the effects of the Prandtl number and the radius ratio on heat transfer coefficient were investigated. The Prandtl number and diameter ratio are each

varied over several orders of magnitude ($0.001 \le Pr \le 1000$, $1.0 \le RR \le \infty$). Cho et al. [3] used a bi-polar coordinate system to investigate the local and overall heat transfer between concentric and eccentric horizontal cylinders for Rayleigh numbers less than 5×10^4 (based on gap width, L). They found that the very small eccentricity gives an overall thermal behavior similar to that of the exactly concentric cylinders. Farouk and Güceri [4] applied a turbulence model to study the turbulent natural convection for high Rayleigh numbers ranging from 10^6 to 10^7 with a radius ratio of 2.6. They also accounted for the buoyancy effects on the turbulence structure. The results for both the laminar and turbulent cases were in good agreement with results obtained experimentally by other investigators. Hessami et al. [5] and Mahony et al. [6] investigated the effect of variable properties on natural convection in horizontal annulus. They found that the Boussinesq approximation is valid for a temperature difference ratio $\varepsilon = \frac{T_h - T_c}{T_c} <$ 0.1. It also can be used for a ratio of ε up to 0.2 with reasonable accuracy in the calculated heat transfer. They also found that the Boussinesq approximation does overestimate the tangential velocity and the temperature gradient near the hot inner cylinder. Tsui et al. [7] investigated numerically and experimentally the transient natural convection between two concentric isothermal cylinders. They covered Grashof numbers from approximately 1×10^3 to 9×10^4 and diameter ratios from 1.2 to 2.0. Several authors such as Takata et al. [8] and Feirao et al. [9] have carried out numerical investigations on the three dimensional convective flow. Feirao et al. [9] considered the steady convection in a wide gap annulus and found that nearly two-dimensional crescent eddies establish in the central region and that the fluid particles move along a coaxial double helix. Hessami et al. [10] investigated experimentally and theoretically the effect of changing the fluid properties within the annulus. They used air, glycerin and mercury in the ranges of $0.023 \le Pr \le 10000$ and $0.03 \le Gr \le 3\times10^6$, and showed that glycerin is more sensitive to the constant properties assumption, while air had not been significantly affected by this assumption. This is due to the large radii ratio they used (RR=11.4). Finally their experimental data have been correlated with some other data from the literature for smaller values of RR . It has been shown that the heat transfer from the inner cylinders should be almost the same as that in an infinite medium when RR ≥10. Kolesnikov and Bubnovich [11] studied numerically a conjugate problem of natural convection in a horizontal annulus and compared the solution with non-conjugate problems. Kumar [12] presented the numerical results for constant heat flux at the inner cylinder and isothermal condition at the outer cylinder. A lower effective sink temperature is obtained when it is compared to isothermal heating, thus a higher heat transfer rate is expected. Choi and Kim [13] studied the linear stability of the crescent-shaped convection of air (Pr = 0.71) by solving the linear equation for three-dimensional disturbances with a time marching method. It was shown that the principle of exchange of stabilities is valid for $d_i/L \ge 2.1$, which implies that the resultant three-dimensional spiral flow is not periodic in time for d_i/L=2.1. Most of the past research has focused on the heat transfer at the surface of cylinders as given in [2]. Recently, Yoo [14, 15] considered the natural convection problem in a narrow horizontal annulus, and investigated the effect of the Prandtl number on the stability of conduction regime and transition of flow patterns. Yoo [16] investigated the flow patterns and bifurcation phenomena for fluids of $0.3 \le Pr \le 1$, in a wide-gap annulus of d_i/L=2. He found that when Ra exceeds a critical value, two kinds of flow patterns are realized according to initial conditions, and two kinds of bifurcation phenomena are observed, which are dependent on the Prandtl number. The origins of the change of flow patterns and dual steady solutions for the convection were clarified by Mizushima et al. [17]. They obtained the whole bifurcation structure of the convection of air (Pr = 0.7) by numerically calculating the stable and unstable steady state solutions and analyzing their linear stability. They concluded that the so-

called " instability " is not an instability of the crescent shaped convection in its strict meaning. It was shown that the transitions of the convection and the appearance of dual stable steady solutions are explained by imperfect trans-critical and saddle-node bifurcations instead of the instability. For natural convection, the Boussinesq approximation simplifies the Navier-stokes equation by neglecting the compressibility effect everywhere except for the buoyancy force terms. Regions of validity of this approximation is presented by Gray and Giorgini [18]. Finally, Kuehn and Goldstein [19] also presented a correlation equation that improved upon previously published results. In all of the numerical studies, the cylinders are assumed to be long, hence the flow is two dimensional, with the inner cylinder hotter than the outer cylinder.

Our basic aim here is to investigate numerically the natural convection heat transfer between two horizontal concentric and isothermal cylinders as to get the complete image about the heat transfer characteristics of this problem.

The present numerical investigations will cover diameter ratios of (1.25-10) and Rayleigh numbers (based on inner diameter, d_i) ranging from 10^2 to 10^6 at Prandtl number = 0.71.

2. Mathematical formulation

In the present study, air between the two concentric cylinders will be considered a Newtonian constant property fluid except for the density in the buoyancy force components existing in the momentum equations. The Boussinesq approximation will relate the variable density to the local temperature.

The steady state dimensionless equations governing the transport of mass, momentum and thermal energy in the cylindrical coordinates (r,ϕ) for the case of incompressible fluid flow are:

$$\frac{\partial V_r}{\partial R}+\frac{V_r}{R}+\frac{\partial V_\phi}{R\partial\phi}=0, \tag{1}$$

$$\left(V_r\frac{\partial V_r}{\partial R}+V_\phi\frac{\partial V_r}{R\partial\phi}-\frac{V_\phi^2}{R}\right)=-\frac{\partial P_d}{\partial R}-\frac{Ra}{8\,Pr}\theta\cos\phi+\left(\frac{\partial^2 V_r}{\partial R^2}+\frac{1}{R}\frac{\partial V_r}{\partial R}-\frac{V_r}{R^2}+\frac{\partial^2 V_r}{R^2\partial\phi^2}-\frac{2}{R^2}\frac{\partial V_\phi}{\partial\phi}\right), \tag{2}$$

$$\left(V_r\frac{\partial V_\phi}{\partial R}+V_\phi\frac{\partial V_\phi}{R\partial\phi}+\frac{V_rV_\phi}{R}\right)=-\frac{\partial P_d}{R\partial\phi}+\frac{Ra}{8\,Pr}\theta\sin\phi+\left(\frac{\partial^2 V_\phi}{\partial R^2}+\frac{1}{R}\frac{\partial V_\phi}{\partial R}-\frac{V_\phi}{R^2}+\frac{\partial^2 V_\phi}{R^2\partial\phi^2}+\frac{2}{R^2}\frac{\partial V_r}{\partial\phi}\right), \tag{3}$$

$$\left(V_r\frac{\partial\theta}{\partial R}+V_\phi\frac{\partial\theta}{R\partial\phi}\right)=\frac{1}{Pr}\left[\frac{1}{R}\frac{\partial}{\partial R}\left(R\frac{\partial\theta}{\partial R}\right)+\frac{\partial^2\theta}{R^2\partial\phi^2}\right], \tag{4}$$

The following dimensionless variables are used:

$$V_r=\frac{v_r}{(\nu/a)},\quad V_\phi=\frac{v_\phi}{(\nu/a)},\quad R=\frac{r}{a},\quad \theta=\left(\frac{T-T_c}{T_h-T_c}\right),$$

$$P_d=\frac{p_d}{\rho(\nu/a)^2},\quad Pr=\frac{Cp\mu}{k},$$

$$\nu=\frac{\mu}{\rho},\quad Ra=\frac{(2a)^3\beta\,g(T_h-T_c)}{\nu\alpha},\quad \text{and}\quad \alpha=\frac{k}{\rho\,c_p}. \tag{5}$$

The above equations are subjected to the following boundary conditions:

at $R=1$ and $0\le\phi\le\pi$:

$$V_R=V_\phi=0,\ \theta=1, \tag{6-a}$$

at $R=\frac{R_o}{R_i}$ and $0\le\phi\le\pi$:

$$V_R=V_\phi=0,\theta=0, \tag{6-b}$$

at $1\le R\le\frac{R_o}{R_i}$ and $\phi=0$ or π:

$$V_\phi=0,\ \frac{\partial V_R}{\partial\phi}=0,\ \frac{\partial\theta}{\partial\phi}=0. \tag{6-c}$$

Since the flow and heat transfer is symmetrical about the vertical axis, it suffices to consider only one half of the flow field on either side of the vertical axis. This is shown in fig. 1.

2.1. The nusselt number

The local Nusselt number, Nu_ϕ is defined as:

$$Nu_\phi = \frac{h_\phi(2a)}{k} = -2\frac{\partial\theta}{\partial R}\Big|_{R=1}. \quad (7)$$

The average Nusselt number, Nu over the inner cylinder perimeter is defined as:

$$Nu = \frac{h(2a)}{k} = \frac{-2}{\pi}\int_0^\pi \frac{\partial\theta}{\partial R}d\phi = \frac{-2}{\pi}\sum_0^\pi \left(\frac{\partial\theta}{\partial R}\right)_{R=1}\Delta\phi. \quad (8)$$

2.2. The calculation grid

The number of nodes for the solution in the half annular space was taken as 50 nodes in the radial direction and 90 nodes in the circumferential direction. The spacing between the nodes in the circumferential direction was taken uniform. However, in the radial direction, non- uniform spacing was used for better accuracy, with smaller spacing near each of the two cylinders.

3. The numerical solution

The governing eqs. (1-4) along with the boundary conditions given by eqs (6-a, 6-b and 6-c) can not be solved analytically. So, the numerical methods remain the only possible solution one could take. The computer program used to solve the above equations is based on the finite difference technique developed by Patankar [20]. This was based on the discretization of the governing equations using the central differencing in space. The discretization equations were solved by the Gauss-seidel elimination method. The iteration method used in this program is a line by line procedure, which is a combination of the direct method and the resulting Tri Diagonal Matrix Algorithm (TDMA). The procedure used by Patankar is to solve simultaneously the continuity and momentum equations then the thermal energy equation. The accuracy of the solution and the number of iterations were checked. The iteration is stopped according to a certain tolerance in the variation of the value of the Nusselt number. So, the accuracy was defined by the change in the average Nusselt number through one hundred iterations to be less than 0.01% from its value. This check showed that 1500 iterations were enough for the required accuracy.

4. Results

Before proceeding with the numerical solutions, the numerical method and the computer program were checked for the case of pure conduction in the present configuration. This is done by solving only the energy equation alone with the given boundary conditions. Other equations (continuity and momentum equations) are ignored in the numerical solution.

As shown in eqs. (4, 6), the pure conduction solution depends only on the radius ratio and is independent of the Rayleigh or Prandtl numbers. The exact value for the average Nusselt number for pure conduction between two isothermal concentric cylinders is derived from the analytical solution of the energy equation. It is given as:

$$Nu = \frac{2}{Ln(RR)}. \quad (9)$$

The numerical values of the conduction solution for $1.25 \le RR \le 10$ are exactly the same as the analytical values given by eq. (9).

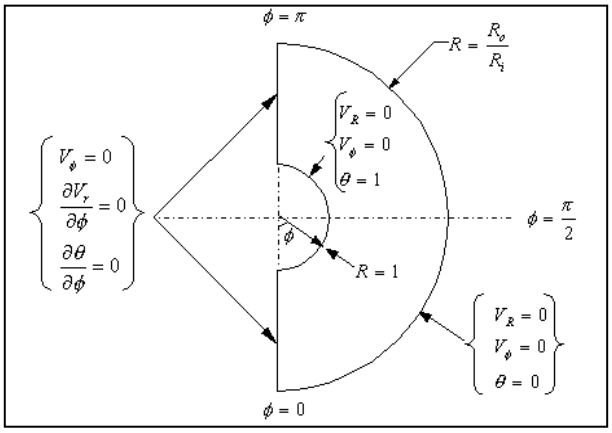

Fig.1. Boundary conditions of the natural convection problem.

4.1. Streamlines and isotherms

The streamlines and isotherms for the flow between the two concentric horizontal cylinders due to natural convection are plotted with the aid of the Surfer software version 6.01 in figs. 2 up to 5. The results in these figures are obtained at different fixed values of Rayleigh numbers between 10^2 and 10^6, and the radius ratio was varied from 1.25 to 10.

4.1.1. Isothermal lines

For low Rayleigh numbers (Ra=10^2), the isotherms for $RR \leq 5$ consist of concentric cylinders approaching the inner hot cylinder as RR increases. This indicates that conduction heat transfer regime prevails in these cases. For RR >5, the boundary layer regime is dominant with the isotherms concentrated at the hot inner cylinder. The lower part of the annular gap is not affected by the flow.

For high Rayleigh numbers (Ra=10^6), the flow changes from the conduction regime (at RR=1.25) to the boundary layer regime for $RR \geq 2$. As the radius ratio increases; a stratified region is developed in the middle region between the two cylinders (figs. 4-b and 5-b). This leaves the lower part below the hot cylinder almost unaffected by the flow.

4.1.2. Streamlines

For low Rayleigh numbers (Ra=10^2), the flow consists of a big single cell filling the whole domain with its center of rotation moving upwards as the radius ratio is increased from 1.25 to 10 . For high Rayleigh numbers (Ra=10^6), the conduction flow at RR=1.25 changes continuously to the boundary layer regime with the streamlines getting closer to the cylinder surfaces. The lower part of the annular gap becomes more and more stagnant as the radius ratio increases above RR=2. For $RR \geq 5$, the flow takes the shape of a plume where the streamlines are concentrated around the inner hot cylinder and the flow is entrained and raised above the top of the hot cylinder, then falls down along the cold cylinder.

4.2. The average nusselt number

Fig. 6-a shows the average Nusselt number versus the radius ratio for Pr =0.71 and fixed different values of the Rayleigh number. It shows that the flow always starts in the conduction regime for low RR (RR=1.25) and low Ra (Ra =10^2). As the radius ratio increases, the gap thickness increases, thus the conduction Nusselt number decreases. A plot of the conduction Nusselt number is shown on the same figure as given by eq. (9). This decrease in Nu continues until the free convection starts in the gap and thus Nu starts to increase. The onset of convection depends on the values of Ra and RR. As Ra increases from 10^2, convection starts earlier at higher values of the radius ratio. This is clearly shown in fig. 6-b where conduction Prevails for RR=1.25 up to Ra =10^6. However, the convection started at Ra = 10^4 for RR=2, and Ra = 10^3 for RR=2.6. For $RR \geq 5$ the convection was already dominant at Ra = 10^2.

4.3. Local nusselt number

The distribution for local Nusselt number along the hot cylinder, Nu_ϕ for Pr =0.71 and $10^2 \leq Ra \leq 10^6$ for different values of RR in the range $1.25 \leq RR \leq 10$ is given in fig. 7. For RR=1.25, the conduction regime (Nu_ϕ is constant along the cylinder surface) prevails for Ra <10^5. At Ra =10^5, the free convection starts and the local Nusselt number is maximum at the bottom of the inner hot cylinder (ϕ =0°). As the angle, ϕ increases, Nu_ϕ monotonically decreases up to a location where flow separation occurs at $\phi \cong 165°$. The local Nusselt number starts to increase after separation till ϕ =180°.

For RR>1.25, the same behavior occurs except that the conduction regime ends at lower values of Ra and for $RR \geq 5$, convection is dominant for Ra >10^2.

4.4. Velocities and temperature distributions

The angular and radial velocities and temperature distributions along a radius in the annular gap at ϕ = 90° are shown in fig. 8 for Pr =0.71, and RR =2 in the Rayleigh number range $10^2 \leq Ra \leq 10^6$.

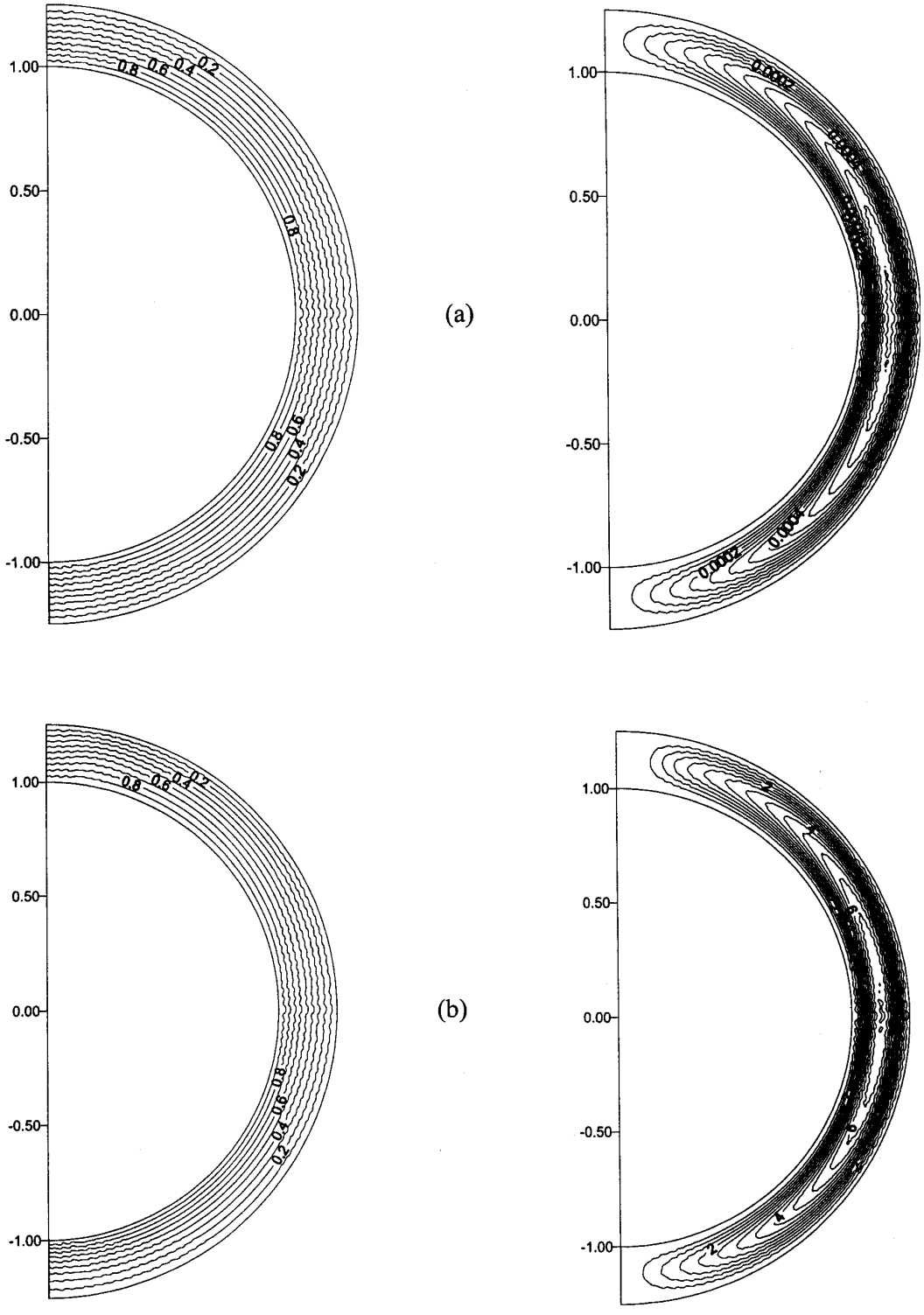

Fig. 2. Isotherms (left) & Streamlines (right) for Pr=0.71, RR=1.25 (a) Ra=10^2, (b) Ra=10^6.

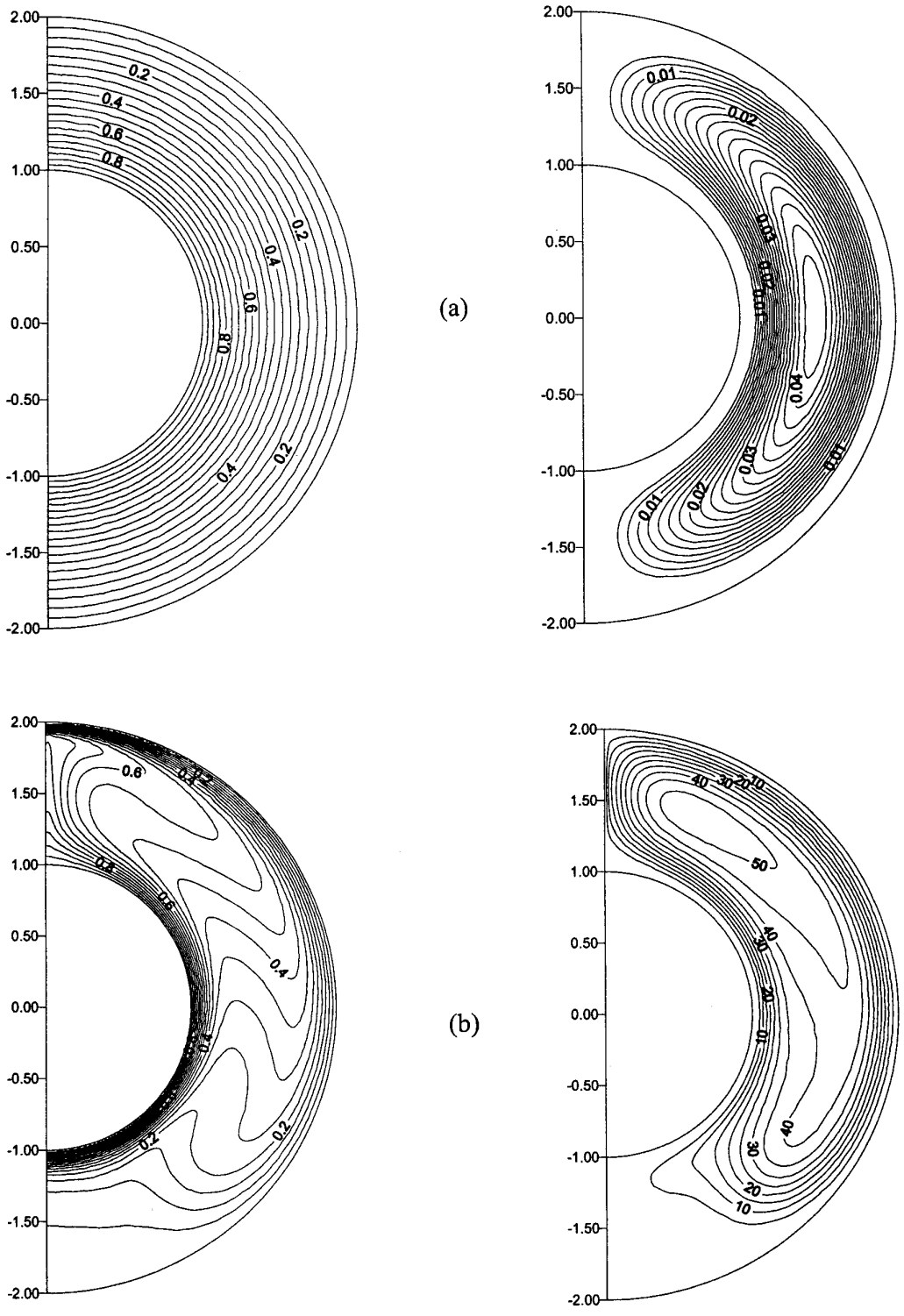

Fig. 3. Isotherms (left) & Streamlines (right) for Pr=0.71, RR=2 (a) Ra=10^2, (b) Ra=10^6.

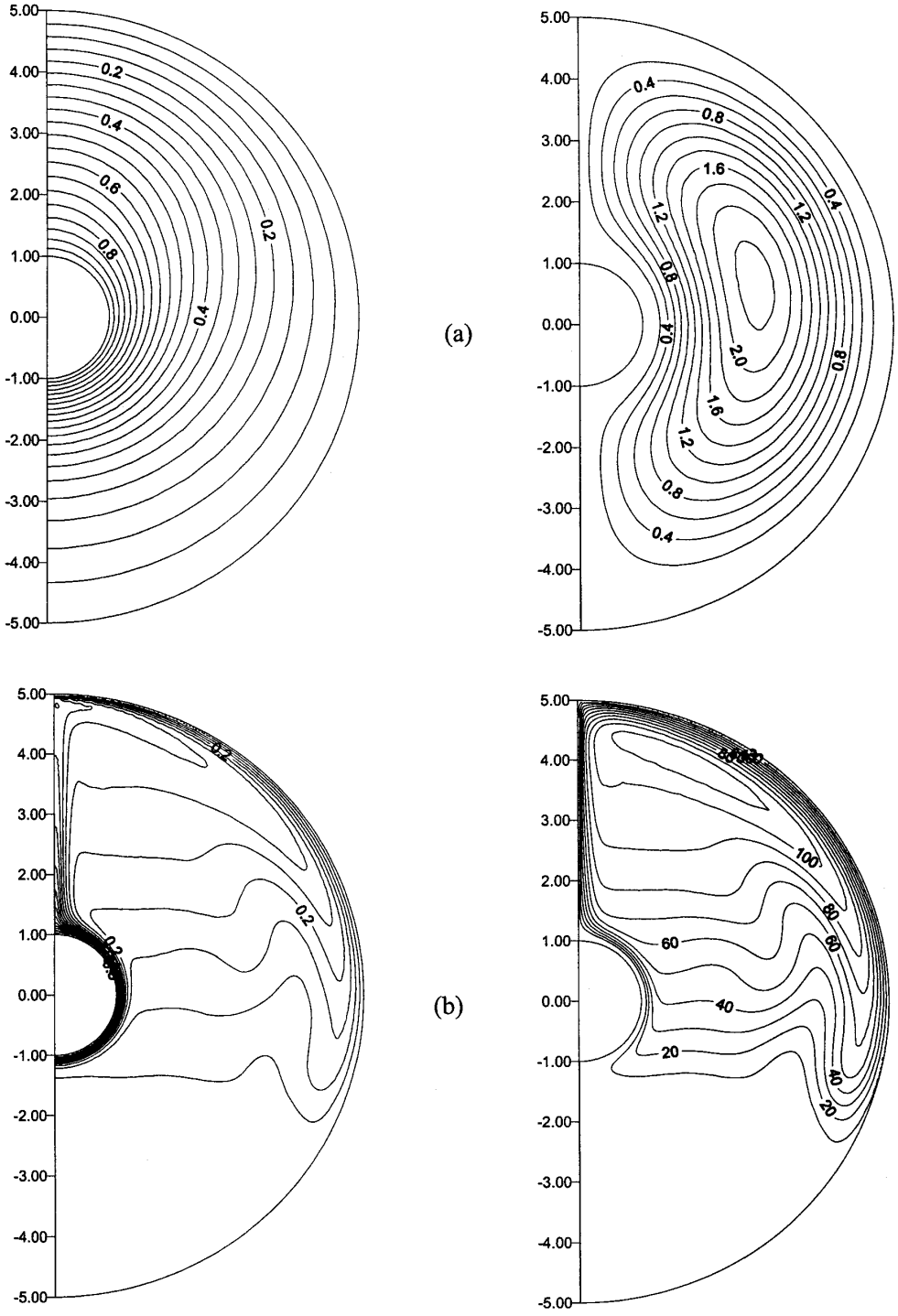

Fig. 4. Isotherms (left) & Streamlines (right) for Pr=0.71, RR=5 (a) Ra=10^2, (b) Ra=10^6.

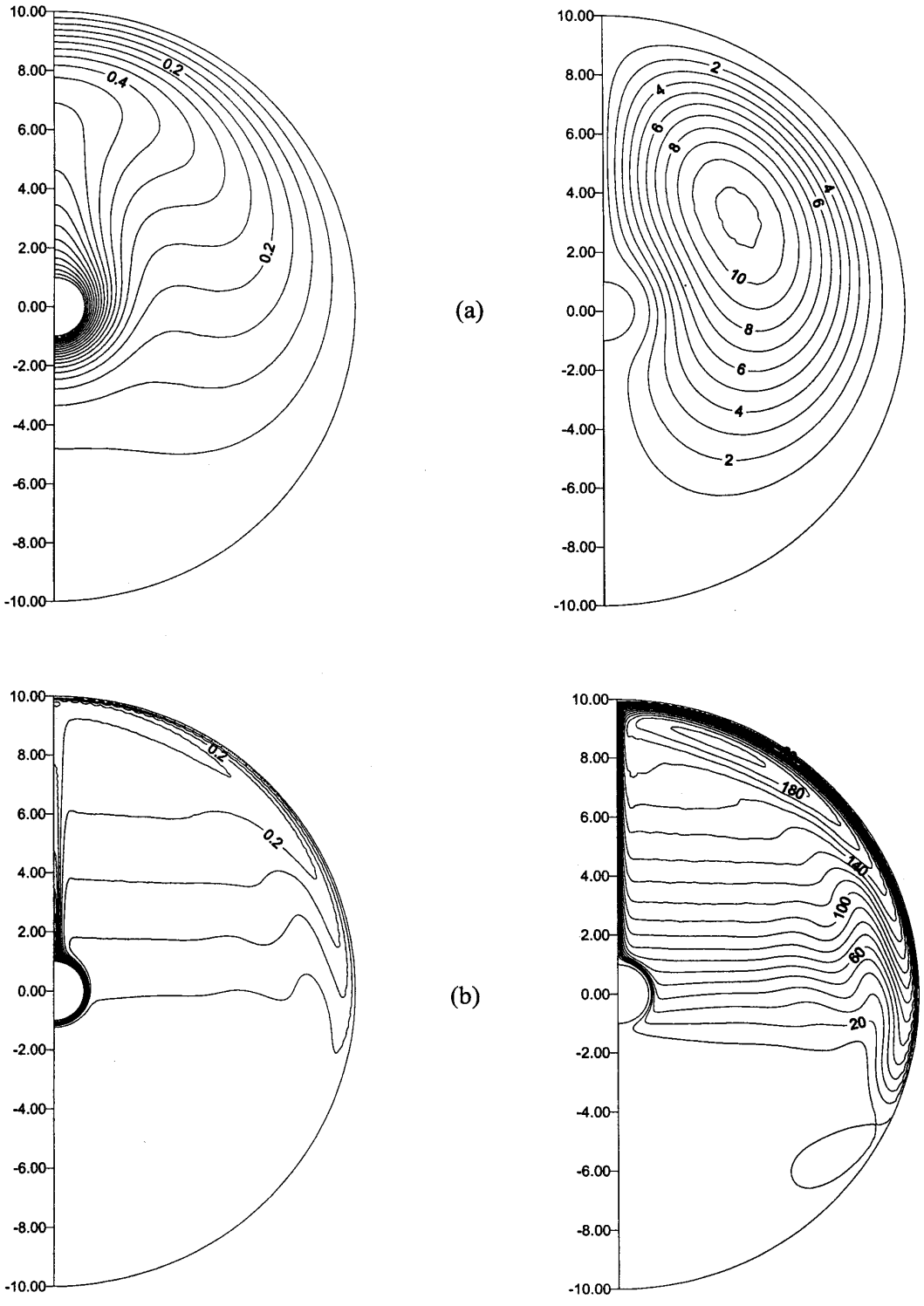

Fig. 5 Isotherms (left) & Streamlines (right) for Pr=0.71, RR=10 (a) Ra=10^2, (b) Ra=10^6.

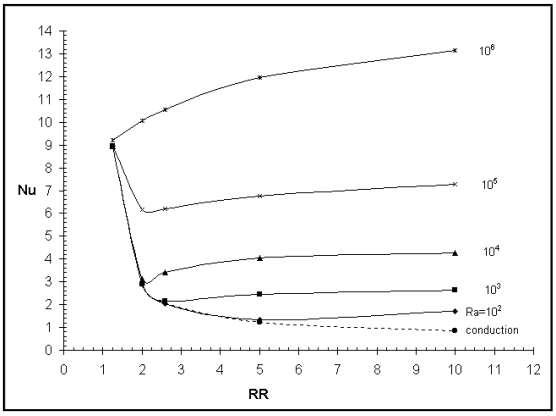

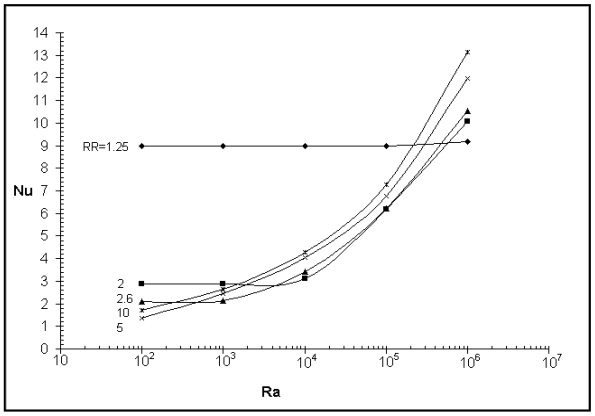

Fig. 6. Average Nusselt number for *Pr*=0.71.

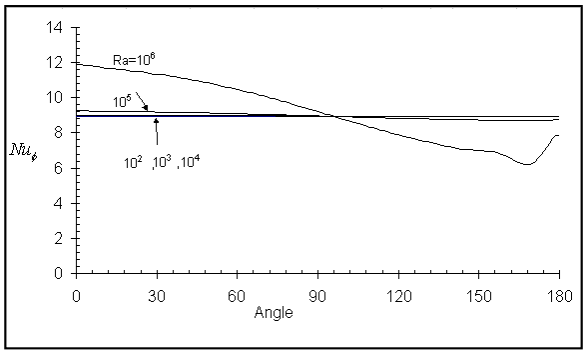

(a) *RR*=1.25

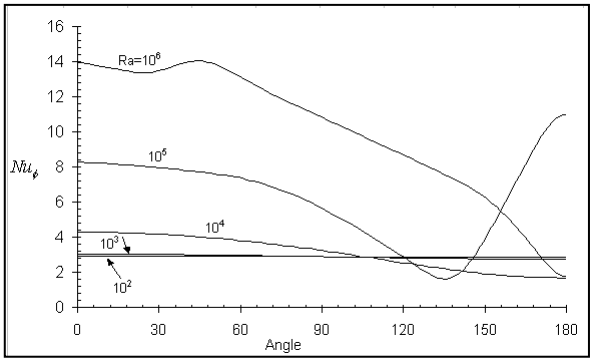

(b) *RR*=2

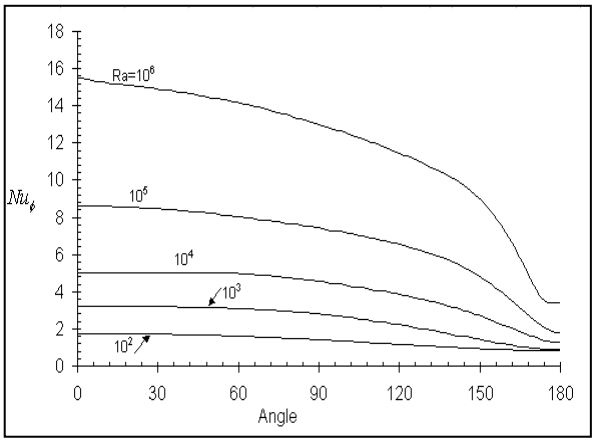

(c) *RR*=5

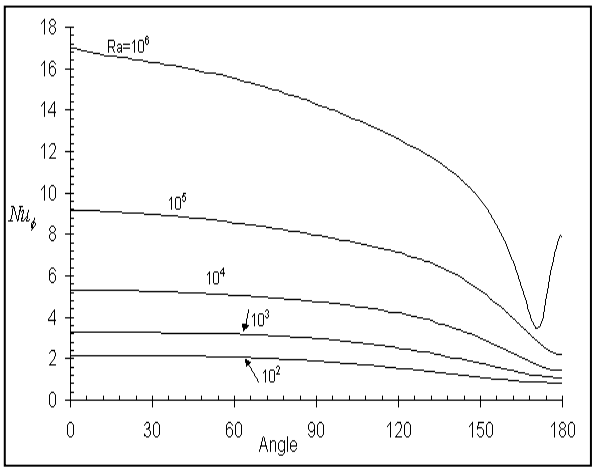

(d) *RR*=10

Fig. 7 Local Nusselt number distribution for *Pr* =0.71.

The dimensionless angular velocity, V_ϕ is very small for $Ra \leq 10^3$ since the flow is dominated by the conduction regime. For $Ra > 10^4$, the laminar boundary layer regime prevails and the location of maximum or minimum velocities moves closer to the cylinder surfaces. This indicates thinner boundary layer thickness as Ra increases. The absolute value of maximum angular velocity near the hot inner cylinder is higher than its value near the cold outer cylinder. This shows that the flow speeds up near the hot cylinder.

The distribution of the dimensionless radial velocity, V_r is given in fig. 8-b. It shows that its value increases with Ra. It is in general directed towards the center of the cylinders except for $Ra = 10^5$ in a small region near the hot cylinder.

The dimensionless temperature distribution, θ is shown in fig. 8-c. For $Ra \leq 10^4$ it is logarithmic distribution as the flow is in the conduction regime. For $Ra \geq 10^5$, the laminar boundary layer regime prevails and the temperature change concentrates near the two cylindrical walls with higher temperature rates at higher Ra. The core of the annular gap is almost isothermal and the temperature drop is higher near the inner hot cylinder.

To study the effect of the radius ratio on the distributions, fig. 9 shows the velocities and temperature distributions for Pr =0.71 and RR=10. From figs. 8 and 9, increasing RR moves the flow quickly to the boundary layer regime with higher velocities at higher Ra. The magnitude of the radial velocities increased with RR and the laminar boundary layer was more confined near the hot inner cylinder where most of the temperature drop occurs. The temperature is almost constant over a large part of the middle portion of the annular gap.

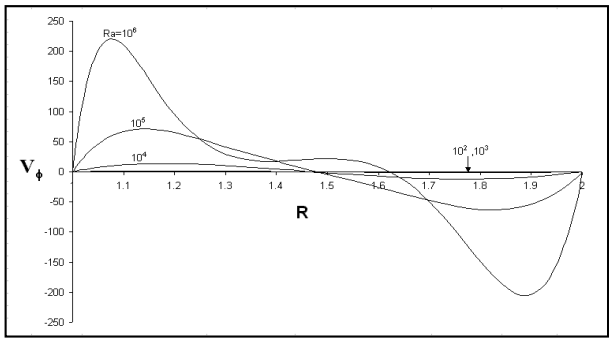

(a) Angular velocity component

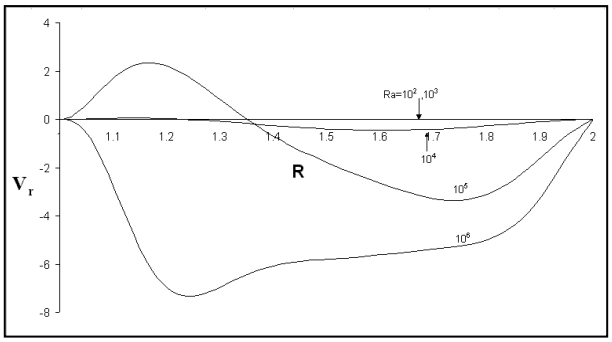

(b) Radial velocity component

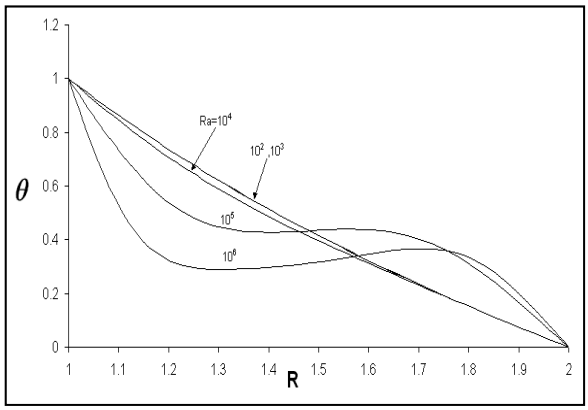

(c) Temperature distribution

Fig. 8. Velocities and Temperature distributions along a radius for Pr =0.71, RR=2, ϕ =90°.

5. Correlations and comparison with previous work

The correlating method suggested by Churchill and Chu [21] is used and the form of correlation given by Kuehn and Goldstein [2] is adapted. The Least- Squares method is used to get the optimum constants of the correlations which are given as:

$$Nu = \left(Nu_{cond}^{15} + Nu_{conv}^{15} \right)^{1/15}, \qquad (10\text{-a})$$

where,

$$Nu_{cond} = \frac{2}{Ln(RR)}. \qquad (10\text{-b})$$

$$Nu_{conv} = \frac{2}{Ln\left[\dfrac{1 + 6.659\, Ra^{-0.294}}{1 - 2.441 \left(Ra \,.\, RR^3 \right)^{-0.206}} \right]}. \qquad (10\text{-c})$$

The numerical results along with the correlations are shown in fig. 10. The maximum deviation is 7 % and the standard deviation is about 0.014. A comparison with previous work for *RR*=2.6 is shown in fig. 11. A good agreement is shown with a maximum deviation of 9.6 %.

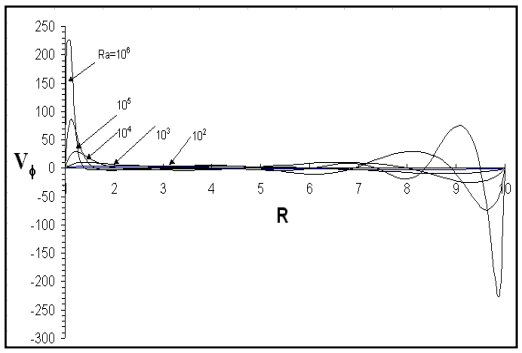

(a) Angular velocity component

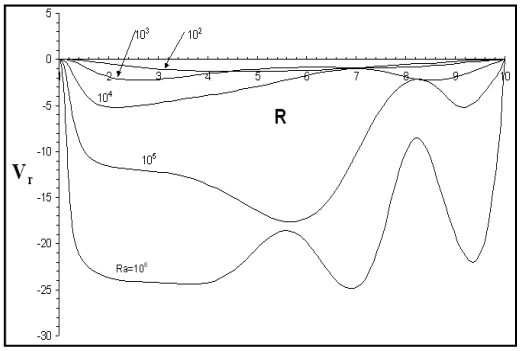

(b) Radial velocity component

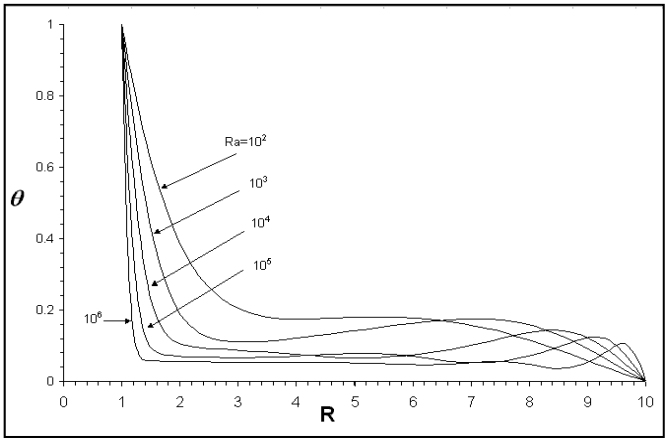

(c) Temperature distribution

Fig. 9. Velocities and temperature distributions along a radius for *Pr* =0.71, *RR*=10, ϕ =90°.

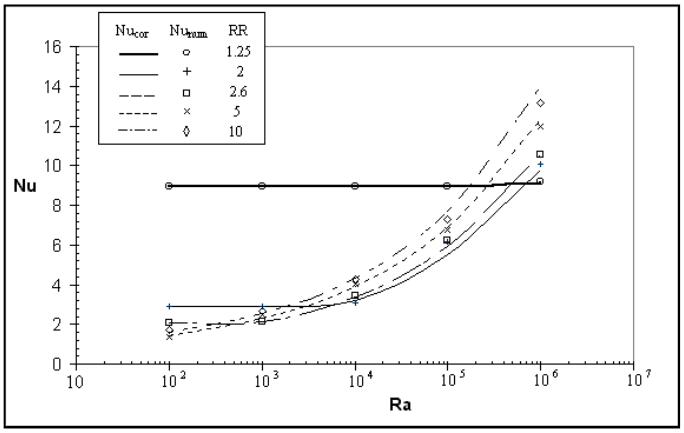

Fig. 10. Comparison between correlation Nusselt number and numerical Nusselt number for Pr =0.71.

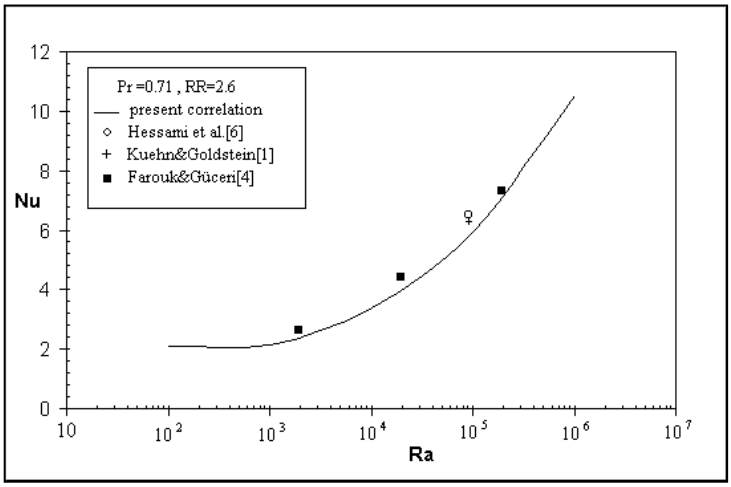

Fig. 11. Comparison between correlation and previous data.

6. Conclusions

Laminar natural convection in the air annular gap between two infinite horizontal isothermal cylinders is numerically studied. The study covered a wide range of Ra from 10^2 to 10^6 and the radius ratio changed between 1.25 and 10. A computer program is developed to solve the governing equations. It was initially checked for the problem of pure conduction in the annular gap where the numerical and analytical solutions were exactly the same. Streamlines and isotherms are presented as well as average and local Nusselt numbers. Also, velocity and temperature distributions are given. The study shows that the annular gap can represent a single inner cylinder in an infinite medium for RR=10 if $Ra \leq 10^5$. For higher Ra, the radius ratio should be increased much over 10. For $Ra \leq 10^2$ and $RR \leq 5$, the flow represents pure conduction. The laminar boundary layer regime starts at higher Ra or larger RR. A correlation equation is given by eq. (10) where a good agreement is shown between present and previous work with a maximum deviation of 9.6 %.

Nomenclature

a is the radius of inner hot cylinder , ($a = r_i r_i$) , m,
c_p is the specific heat , J/kgK,
d_i is the diameter of inner cylinder ,

(d_i=2a) , m,

g is the gravitational acceleration , m/s^2 ,

Gr is the Grashof number, $g\beta(T_h - T_c)(2a)^3/\nu^2$,

h is the average heat transfer coefficient, W/m^2K,

h_ϕ is the local heat transfer coefficient, W/m^2K,

k is the thermal conductivity, W/mK,

L is the gap width, $(r_o - r_i)$, m ,

Nu is the average Nusselt number, $h(2a)/k$,

Nu_ϕ is the local Nusselt number, $h_\phi(2a)/k$,

p_d is the dynamic pressure, N/m^2

P_d is the dimensionless dynamic pressure, $P_d = \frac{p_d}{\rho(\nu/a)^2}$,

Pr is the Prandtl number, $\mu c_p/k$,

r is the radial coordinate, m,

r_i is the radius of inner cylinder, m,

r_o is the radius of outer cylinder, m.

R is the dimensionless radial coordinate, r/a,

RR is the radius ratio, r_o/r_i,

Ra is the Rayleigh number based on inner diameter $g\beta(T_h - T_c)(2a)^3/\nu\alpha$,

T is the local fluid temperature, K,

T_h is the temperature of hot inner cylinder, K.

T_c is the temperature of cold outer cylinder, K.

v_r is the radial velocity , m/s,

V_r is the dimensionless radial velocity,

v_ϕ is the angular velocity , m/s, and

V_ϕ is the dimensionless angular velocity.

Greek symbols

α is the thermal diffusivity , $k/c_p\rho$, m^2/s,

β is the coefficient of volumetric thermal expansion, K^{-1} ,

ρ is the local density, kg/m^3 ,

μ is the dynamic viscosity, kg/ms,

ν is the kinematic viscosity, μ/ρ , m^2/s,

ϕ is the angular coordinate, rad, and

θ is the dimensionless temperature, $(T - T_c)/(T_h - T_c)$.

Subscripts

c is the cold,

h is the hot,

i is the inner, and

o is the outer.

References

[1] T.H. Kuehn and R.J. Goldstein, "An Experimental and Theoretical Study of Natural Convection in The Annulus Between Horizontal Concentric cylinders", J. Fluid Mech., Vol. 74 (4), pp. 695-719 (1976).

[2] T.H. Kuehn and R.J. Goldstein, "A Parametric Study of Prandtl Number and Diameter Ratio Effects on Natural Convection Heat Transfer in Horizontal Cylindrical Annuli", J. Heat Transfer, Vol. 102, pp. 768-770 (1980).

[3] C.H. Cho, K.S. Chang and K.H. Park, "Numerical Simulation of Natural Convection in Concentric and Eccentric Horizontal Cylindrical Annuli", J . Heat Transfer, Vol. 104, pp. 624-630 (1982).

[4] B. Farouk and S.I. Güceri, "Laminar and Turbulent Natural Convection in the Annulus Between Horizontal Concentric Cylinders", J. Heat Transfer, Vol. 104, pp. 631-636 (1982).

[5] M.A. Hessami, A. Pollard and R.D. Rowe, "Numerical Calculation of Natural Convective Heat Transfer Between Horizontal Concentric Isothermal Cylinders- Effects of the Variation of the Fluid Properties", ASME J. Heat Transfer, Vol. 106, pp. 668-671 (1984).

[6] D.N. Mahony, R. Kumar and E.H. Bishop, "Numerical Investigation of Variable Property Effects on Laminar Natural Convection of Gases Between

Two Horizontal Isothermal Concentric Cylinders", J. Heat Transfer, Vol. 108, pp. 783 –789 (1986).

[7] Y.T. Tsui and B. Tremblay, "On Transient Natural Convection heat Transfer in the Annulus Between Concentric, Horizontal Cylinders with Isothermal Surfaces", Int. J. Heat Mass Transfer, Vol. 27 (1), pp. 103-111 (1984).

[8] Y. Takata, K. Iwashige, K. Fukuda and S. Hasegawa, "Three–Dimensional Natural Convection in an Inclined Cylindrical Annulus", Int. J. Heat Mass Transfer, Vol. 27 (5), pp. 747-754 (1984).

[9] Y.F. Rao, Y. Miki, K. Fukuda, Y. Takata and S. Hasegawa, "Flow Patterns of Natural Convection in Horizontal Cylindrical Annuli", Int. J. Heat Mass Transfer, Vol. 28 (3), pp. 705-714 (1985).

[10] M.A. Hessami, A. Pollard, R.D. Rowe and D.W. Ruth, "A Study of Free Convective Heat Transfer in a Horizontal Annulus with a Large Radii Ratio", J. Heat Transfer, Vol. 107, pp. 603-610 (1985).

[11] P.M. Kolesnikov and V.I. Bubnovich, "Non-Stationary Conjugate Free–Convective Heat Transfer in Horizontal Cylindrical Coaxial Channels", Int. J. Heat Mass Transfer, Vol. 31 (6), pp. 1149-1156 (1988).

[12] R. Kumar, "Study of Natural Convection in Horizontal Annuli", Int. J. Heat Mass Transfer, Vol. 31 (6), pp. 1137-1148 (1988).

[13] J.Y. Choi and M.U. Kim, "Three-Dimensional Linear Stability of Natural Convection Flow Between Concentric Horizontal Cylinders", Int. J. Heat Mass Transfer, Vol. 36 (17), pp. 4173-4180 (1993).

[14] J.S. Yoo, "Natural Convection in a Narrow Horizontal Cylindrical Annulus: Pr ≤ 0.3", Int. J. Heat Mass Transfer, Vol. 41, pp. 3055-3073 (1998).

[15] J.S. Yoo, "Transition and Multiplicity of Flows in Natural Convection in a Narrow Horizontal Cylindrical Annulus: Pr=0.4", Int. J. Heat Mass Transfer, Vol. 42, pp. 709-722 (1999).

[16] J.S. Yoo, "Prandtl Number Effect on Bifurcation and dual Solutions in Natural Convection in a Horizontal Annulus", Int. J. Heat Mass Transfer, Vol. 42, pp. 3279-3290 (1999).

[17] J. Mizushima, S. Hayashi and T. Adachi, "Transitions of Natural Convection in a Horizontal Annulus", Int. J. Heat Mass Transfer, Vol. 44, pp. 1249 –1257 (2001).

[18] D.D. Gray and A. Giorgini, "The Validity of the Boussinesq Approximation for Liquids and Gases", Int. J. Heat Mass Transfer, Vol. 19, pp. 545 – 551 (1976).

[19] T.H. Kuehn and R.J. Goldstein, "Correlating Equations for Natural Convection Heat Transfer Between Horizontal Circular Cylinders", Int. J. Heat Mass Transfer, Vol. 19, pp. 1127-1134 (1976).

[20] S.V. Patankar, Numerical Heat Transfer and Fluid Flow, McGraw- Hill, NewYork (1980).

[21] S.W. Churchill and H.H.S. Chu, "Correlating Equations for Laminar and Turbulent free Convection from a Horizontal Cylinder", Int. J. Heat Mass Transfer, Vol. 18, pp. 1049-1053 (1975).

Received December 16, 2003
Accepted February 10, 2004